CrossMark
click for updates

Benzimidazole derivative fluorescent probe for cascade recognition of phosphate and iron ions in aqueous medium and its logic gate behavior†

Liyan Wang,*[a] Ying Tian,[a] Limin Ding,[b] Bing Zhao,[a] Xianyou He,[a] Bo Song[a] and Shifu Liu[a]

A fluorescent probe based on benzimidazole was synthesized, and its cascade recognition of PO_4^{3-} and Fe^{3+} ions was investigated using spectroscopic techniques. This probe showed a highly sensitive and selective response towards PO_4^{3-} and Fe^{3+} relative to other anions and metal ions. Moreover, the resulting [probe–PO_4^{3-}] complex exhibited a turn-off response toward Fe^{3+} ion, leading to the fabrication of an INHIBIT logic gate using PO_4^{3-} and Fe^{3+} ions as inputs and the emission of the probe as output. This research may enrich the field of multi-functional chemosensors in natural products.

1. Introduction

Ionic recognition has drawn great attention in the past decades due to its crucial role in biological, environmental, and chemical fields.[1–5] Although many selective chemosensors have been reported, multi-functional chemosensors that can accomplish cascade recognition by detecting a second analyte based on a coordination complex of a host molecule and the first analyte are relatively rare.[6,7] Therefore, the development of recyclable, cost effective, and high performance sensors for cascade detection is of great interest.

Among the various anions, phosphates, including inorganic species ($H_2PO_4^-$, HPO_4^{2-}, PO_4^{3-}, PP_i) and their derivatives, such as nucleoside polyphosphates (ATP, ADP, and AMP), play a key role in life processes, such as energy storage,[8] gene building[9] and information transfer.[10] However, the adverse effects of excess phosphate in blood also cause some diseases, such as hyperphosphatemia and cardiovascular complications resulting from the development of metastatic calcifications at the cardiac level, and increased morbidity and mortality.[11,12] Considerable effort has focused on designing new chemosensors for the detection of phosphate ions and their derivatives in the last few decades.[13–15] Though numerous materials have been developed to sense phosphate ions, most use metal ion complexes for sensing. For example, Tobey and Anslyn[16] synthesized a copper ion complex for phosphate, and Bartoli and coworkers[17] synthesized mono- and dinuclear fluorescent zinc(II) complexes for di- and triphosphate. Furthermore, many

of the sensors reported require an organic solvent as the sensing medium or are easily affected by hydrogen phosphate, dihydrogen phosphate, and pyrophosphate. For example, Wu and coworkers[18] designed two complexes as novel phosphate ion probes, which detected phosphate in DMSO/HEPES (8 : 2, v/v) buffer, Azath and coworkers[19] developed a colorimetric sensor for phosphate and pyrophosphate anions, and Liao and coworkers[20] developed a novel chemosensor for hydrogen phosphate and dihydrogen phosphate.

Iron is the most abundant transition metal ion in humans and other mammals, and plays important roles in various biological systems.[21,22] However, an imbalanced iron concentration is known to cause severe deleterious effects. For example, an excess accumulation of iron can cause clinical deterioration and often death in patients with severe forms of thalassemia.[23] Therefore, the detection of trace amounts of iron is of critical interest. In recent years, several fluorescent probes for iron ions with high selectivity and sensitivity have been reported.[24] However, many of the reported fluorescent probes need either an organic solvent as the sensing medium; for example, in detecting Fe^{3+} in H_2O/DMSO (1 : 1, v/v) solutions[25] and in H_2O/ACN (1 : 1, v/v) solutions.[26]

Though several studies on PO_4^{3-} and Fe^{3+} ion recognition have been reported, there has been no report of a cascade recognition system that can detect PO_4^{3-} ions first, followed by Fe^{3+} ions. Herein, we exploited a fluorescent probe, **1**, containing an amide H-bonding donor and benzimidazole with better fluorescence properties. Binding with PO_4^{3-} led to the fluorescence of probe **1** switching on. Due to the high binding ability of Fe^{3+} toward PO_4^{3-}, Fe^{3+} can snatch PO_4^{3-} from the [**1**–PO_4^{3-}] complex to form a stable $FePO_4$ complex and fully restore the emission, which can be applied to the further detection of Fe^{3+}. Interestingly, using PO_4^{3-} and Fe^{3+} as chemical inputs and the fluorescence intensity at 409 nm as

[a]*College of Chemistry and Chemical Engineering, Qiqihar University, Qiqihar, 161006, P. R. China. E-mail: wlydlm@126.com*

[b]*Cadre Ward, Qiqihaer First Hospital, Qiqihar 161005, P. R. China*

output, probe **1** can be used to mimic an INHIBIT (INH) logic gate.

2. Experimental

2.1 Materials and general methods

Deionized water was used throughout the experiment. All reagents and solvents were obtained from commercial sources and were of analytical grade. Solvents were dried according to standard procedures. The salts and solvents were purchased from Sinopharm Chemical Reagent Co., Ltd (Shanghai, China) or Alfa-Aesar Chemical Co. (USA). NMR spectra of 1,4-benzenedi-[3-(1-pentylbenzimidazole)]-acetylaniline dichloride (**1**) were recorded in DMSO-d$_6$ solution on a Bruker Avance 600 MHz spectrometer. ^{1}H chemical shifts were reported in ppm downfield from tetramethylsilane (TMS), with the solvent resonances used as internal standards, and coupling constants (J) are given in Hz. Mass spectra were recorded on a Waters Xevo UPLC/G2-QTof MS instrument equipped with an electrospray (ESI) ion source. Infrared spectra were performed on a Nicolet AVATAR-750 FTIR spectrometer and samples were prepared as KBr pellets. Melting points were determined using an MPA100 Optimelt Automated Melting Point System and uncorrected. All pH measurements were prepared with a Sartorius basic pH-meter PB-10. UV absorption spectra were determined in 4-(2-hydroxyethyl)-1-piperazine-ethanesulfonic acid (HEPES) solution using a Pgeneral TU-1901 UV-vis spectrophotometer. Fluorescence spectra were recorded on a PerkinElmer LS 55 fluorescence spectrometer.

2.2 General procedure for spectroscopic measurements

All metal ion and anion detections were operated at pH 7.4, maintained with HEPES buffer (10 mM). The 10 μM stock solution of probe **1** was prepared in HEPES. The working solutions of probe **1** were freshly prepared by diluting the concentrated stock solution to the desired concentration prior to spectroscopic measurements. Anion solutions (0.1 M) were obtained from the tetrabutylammonium salt of I$^-$, Cl$^-$, Br$^-$, F$^-$, AcO$^-$, H$_2$PO$_4$$^-$, NO$_3$$^-$, CO$_3$$^{2-}$, HCO$_3$$^-$, SO$_4$$^{2-}$, NO$_2$$^-$, HPO$_4$$^{2-}$, BrO$_3$$^-$, SO$_3$$^{2-}$, HSO$_3$$^-$, SCN$^-$, and PO$_4$$^{3-}$. Metal ion solutions (0.1 M) were obtained from NaCl, KBr, Mg(NO$_3$)$_2$, CaCl$_2$, Cr(NO$_3$)$_3$, FeSO$_4$, Co(NO$_3$)$_2$, NiCl$_2$, Cu(NO$_3$)$_2$, Zn(NO$_3$)$_2$, AgNO$_3$,

Cd(NO$_3$)$_2$, HgCl$_2$, Pb(NO$_3$)$_2$, Ba(NO$_3$)$_2$, Fe(NO$_3$)$_3$, and Al(NO$_3$)$_3$. Compounds were stored in a vacuum desiccator containing self-indicating silica, and dried fully before use. All fluorescence data were recorded with an excitation of 269 nm and the slit widths of excitation and emission were 10 nm. Fluorescence measurements used titration experiments and the volume added did not exceed 3% of the total. After the solution mixture was shaken for 1 min, new spectra were measured. All experiments were performed at room temperature and conducted in triplicate at least.

2.3 Synthesis of probe 1

The synthetic route to probe **1** is shown in Scheme 1. 1,4-Bis (chloroethylamido)benzene (**A**) and *N*-pentyl benzimidazole (**B**) were synthesized using reported methods.[27,28] Characterization results for **1** are given in the ESI.†

A mixture of **A** (0.783 g, 3.0 mmol), **B** (1.412 g, 7.5 mmol), and *N,N*-dimethylformamide (30 mL) in a 100 mL round bottom flask was placed in an oil bath. The reaction mixture was heated until a homogeneous solution was formed. The solution was stirred for 4.5 h at 120 °C under a nitrogen atmosphere. The mixture was cooled to room temperature and a light yellow solid was separated and filtered. The resultant solid was recrystallized from methanol–ethyl acetate (1 : 1, v/v) to afford the pure product, 1.528 g (80.1%) of probe **1**, as a light yellow powder. Mp: 244.4–245.9 °C. ^{1}H NMR (DMSO-d$_6$, 600 MHz, ppm): 11.08 (s, 2H), 9.88 (s, 2H), 8.13–8.14 (m, 2H), 8.06–8.08 (m, 2H), 7.68–7.72 (m, 4H), 7.60 (s, 4H), 5.57 (s, 4H), 4.57 (t, J = 7.2 Hz, 4H), 1.90–1.95 (m, 4H), 1.30–1.37 (m, 8H), 0.87 (t, J = 6.9 Hz, 6H). ^{13}C NMR (DMSO, 150 MHz, ppm): 163.73, 143.89, 134.79, 132.31, 131.17, 127.28, 127.06, 120.23, 114.32, 114.20, 79.68, 79.46, 79.24, 49.53, 47.22, 28.72, 28.27, 22.03, 14.23. Mass (ESI-MS): [M − 2Cl]$^{2+}$, calcd 283.3676, found 283.3718. FTIR (KBr) ν (cm^{-1}): 3406, 3142, 3035, 2959, 2934, 2862, 1687, 1588, 1566, 1513, 1486, 1309 and 751.

3. Results and discussion

3.1 Anion sensing studies using probe 1

The availability of probe **1** as a highly selective probe for PO$_4$$^{3-}$ was investigated using UV-vis absorbance spectra and fluorescence spectra of probe **1** after the addition of other representative
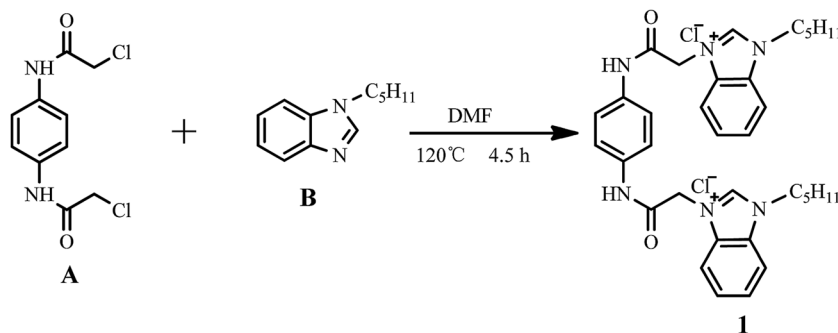
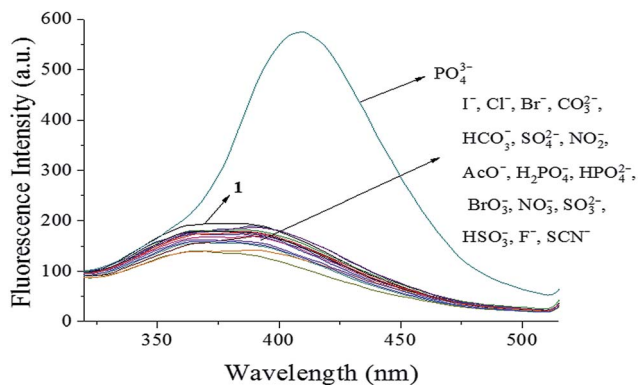**Scheme 1** Synthetic route to **1**.

Fig. 1 Fluorescence spectra of probe 1 (10 μM) upon addition of different anions (1.0 equiv.) in HEPES buffer (10 mM, pH 7.4, 25 °C) solution (λ_{ex} = 269 nm, slit = 10 nm).
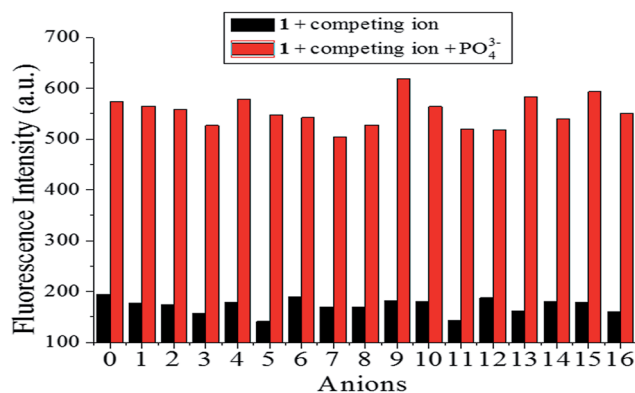

Fig. 2 Fluorescence intensity of probe 1 (10 μM) upon addition of various anions (5.0 equiv.) and PO_4^{3-} (1.0 equiv.) in HEPES buffer (10 mM, pH 7.4, 25 °C) solution (λ_{ex} = 269 nm, slit = 10 nm). (0 is a blank, 1–16 respectively represent (1) I^-, (2) Cl^-, (3) Br^-, (4) CO_3^{2-}, (5) HCO_3^-, (6) SO_4^{2-}, (7) NO_2^-, (8) AcO^-, (9) $H_2PO_4^-$, (10) HPO_4^{2-}, (11) BrO_3^-, (12) NO_3^-, (13) SO_3^{2-}, (14) HSO_3^-, (15) F^-, (16) SCN^-.)

anions (I^-, Cl^-, Br^-, CO_3^{2-}, HCO_3^-, SO_4^{2-}, NO_2^-, AcO^-, $H_2PO_4^-$, HPO_4^{2-}, BrO_3^-, NO_3^-, SO_3^{2-}, HSO_3^-, F^-, and SCN^-). The UV-vis absorbance spectra (Fig. S5†) showed a decrease in absorption intensity at 269 nm soon after PO_4^{3-} addition, while other anions did not induce significant changes. Furthermore, as shown in Fig. 1, only PO_4^{3-} led to an approx. three-fold increase in intensity at 409 nm in the fluorescence spectrum, with a noticeable red shift in emission wavelength observed. Fluorescence emission around 373 nm was not apparent, and only slight quenching was detected, for other anions, indicating the selective sensing behavior of probe 1 toward PO_4^{3-} ions. These results indicated that probe 1 was highly selective toward PO_4^{3-} and might be a potential fluorescent probe for PO_4^{3-} in aqueous solution. Moreover, when L-tryptophan was dissolved in aqueous solution as a reference standard, the fluorescence quantum yield of the [1–PO_4^{3-}] complex was 0.2%, which was higher than that of probe 1 (0.03%). This indicated that the binding of probe 1 and PO_4^{3-} could improve the fluorescence quantum yield.

3.2 Anti-interference of 1 in PO_4^{3-} detection

To further gauge the increased antidisturbance performance of probe 1 toward PO_4^{3-} compared with other anions, competition experiments were carried out by adding 1.0 equiv. PO_4^{3-} to solutions of probe 1 (10 μM) in the presence of 5.0 equiv. of other anions (I^-, Cl^-, Br^-, CO_3^{2-}, HCO_3^-, SO_4^{2-}, NO_2^-, AcO^-, $H_2PO_4^-$, HPO_4^{2-}, BrO_3^-, NO_3^-, SO_3^{2-}, HSO_3^-, F^-, and SCN^-), and fluorescence spectra were recorded, as shown in Fig. 2. The added competing ions had a negligible influence on the fluorescence maxima of the [1–PO_4^{3-}] solutions, which indicated the excellent antidisturbance performance of probe 1 in monitoring PO_4^{3-}.

3.3 Fluorescent titration of PO_4^{3-}

To investigate the PO_4^{3-} ion binding ability of probe 1, fluorescence titration of probe 1 with varying PO_4^{3-} concentration (0–1.5 equiv.) was carried out. As shown in Fig. 3, as the PO_4^{3-} concentration increased, at λ_{ex} = 269 nm the fluorescence intensity increased gradually, accompanied by a red shift and narrowing. Using 1.0 equiv. of PO_4^{3-} enhanced the emission of
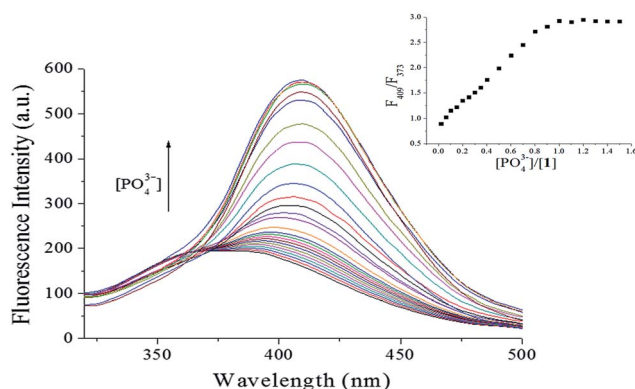

Fig. 3 Fluorescence intensity changes of 1 (10 μM) at various PO_4^{3-} concentrations (0–1.5 equiv.) in HEPES buffer (10 mM, pH 7.4, 25 °C) solution (λ_{ex} = 269 nm, slit = 10 nm). Insets: plot of fluorescence intensity ratio (F_{409}/F_{373}).

probe 1 significantly in the fluorescence titration data due to formation of the [1–PO_4^{3-}] complex. Fluorescence intensity has a linear response toward PO_4^{3-} in the PO_4^{3-} concentration range of 0–1.0 μM, with the linear equation found to be $Y = 161.8002 + 62.6713X$ (linearly dependent coefficient: R^2 = 0.9989), as shown in Fig. 4. The detection limit derived from the fluorescent titration was 0.60 nM with 3σ/slope.[29] The results suggested that probe 1 detected PO_4^{3-} qualitatively with high sensitivity. Furthermore, the binding constant of probe 1 with PO_4^{3-}, which was obtained from fluorescence titration data using the Benesi–Hildebrand equation,[30,31] was 2.3×10^5 M^{-1}, as shown in Fig. 5.

3.4 Effect of pH

To eliminate disturbance from protonation or deprotonation of the fluorophore during detection, the effect of pH on the fluorescence signal of probe 1 in the absence and presence of PO_4^{3-} was studied. As shown in Fig. 6, with increasing pH from 2.0 to
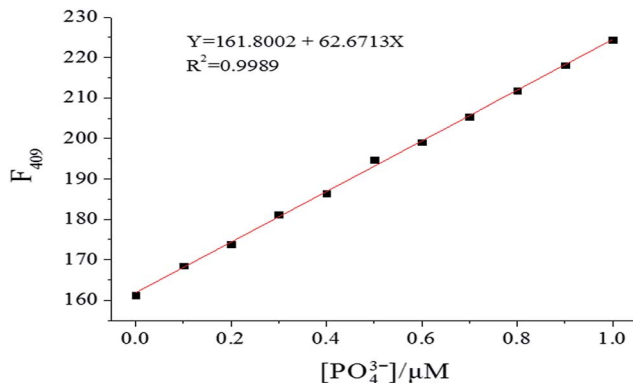
Fig. 4 Fluorescence intensity changes of **1** (10 μM) upon gradual addition of PO_4^{3-} in HEPES buffer (10 mM, pH 7.4, 25 °C) solution (λ_{ex} = 269 nm, slit = 10 nm).
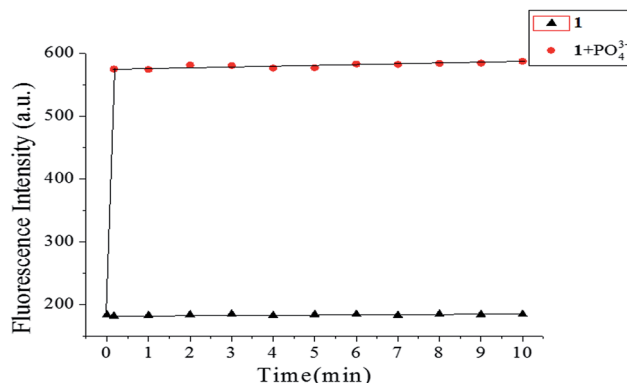

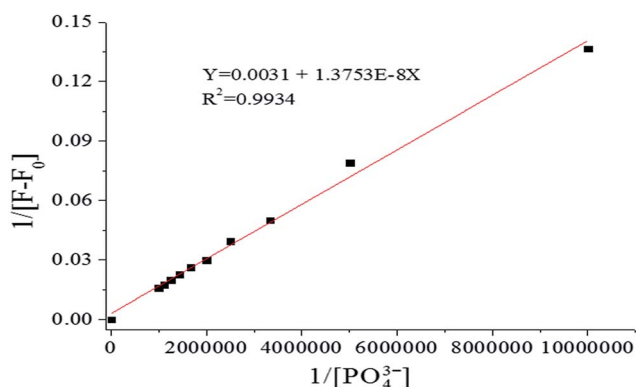Fig. 5 Benesi−Hildebrand plot from fluorescence titration data of **1** (10 μM) in HEPES buffer (10 mM, pH 7.4, 25 °C) solution (λ_{ex} = 269 nm, slit = 10 nm).
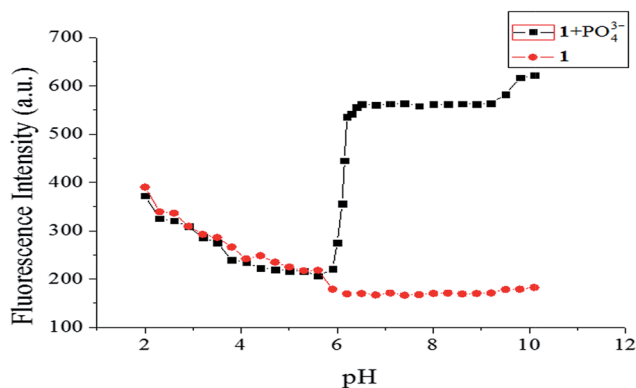

Fig. 6 Fluorescence intensity of probe **1** (10 μM) at different pH values in the absence/presence of PO_4^{3-} (1.0 equiv.).

5.9, the fluorescence intensities almost overlapped, with the dominant forms of phosphate anions likely to be $H_2PO_4^-$ and HPO_4^{2-}.[32,33] Taking the changes in the fluorescence spectra into consideration, probe **1** showed high selectivity for PO_4^{3-} over other anions. Therefore, the combination of probe **1** and PO_4^{3-} was very weak in acidic environments. From pH 5.9 to 6.5, the

Fig. 7 Time-dependent fluorescence intensity of free probe **1** (10 μM) and probe **1** (10 μM) with 1.0 equiv. of PO_4^{3-} in HEPES buffer (10 mM, pH 7.4, 25 °C) solution.

results were very different, showing a rapid increase in the fluorescence emission of probe **1** in with the presence of 1.0 equiv. PO_4^{3-}. However, strong fluorescence was observed from the solution of probe **1** with PO_4^{3-} in the pH range 6.5–10.1, which implied the potential application of probe **1** at environmental and physiological pH values.

3.5 Time-dependence of detection

Time is an important parameter for reaction-based probes. The time-dependent fluorescence of probe **1** (10 μM) using 1.0 equiv. of PO_4^{3-} was studied by monitoring the fluorescence intensity *vs.* time, as shown in Fig. 7. Upon addition of PO_4^{3-} to the solution of probe **1**, the fluorescence intensity increased rapidly, reaching a maximum within 10 s, and then approximately leveling off, while that of the probe **1** solution alone was stable at a very low level. These results indicated that probe **1** was sensitive and reliable, and that PO_4^{3-} detection can be completed within minutes.

3.6 Mechanism for PO_4^{3-} sensing using 1

To confirm the stoichiometry of binding between probe **1** and PO_4^{3-} ions, Job's plots analysis was carried out. As shown in Fig. 8, the maximal increment of fluorescence intensity between **1** and [**1**–PO_4^{3-}] appeared at a PO_4^{3-} molar fraction of 0.5. According to the equation $n = x/(1 - x)$,[34] in which x is the molar fraction of PO_4^{3-}, corresponding to the maximal fluorescence change and n is the binding stoichiometry, 0.5 indicated a binding stoichiometry for **1** and PO_4^{3-} of 1 : 1.

This 1 : 1 stoichiometry was further confirmed by ESI-MS results. A series of peaks at m/z 679.5204 corresponding to $[\mathbf{1}^{2+} + PO_4^{3-} + 4H^+ + H_2O]^{3+}$, 701.4925 corresponding to $[\mathbf{1}^{2+} + PO_4^{3-} + 3H^+ + H_2O + Na^+]^{3+}$, 715.3033 corresponding to $[\mathbf{1}^{2+} + PO_4^{3-} + 4H^+ + H_2O + Cl^-]^{2+}$, 737.2858 corresponding to $[\mathbf{1}^{2+} + PO_4^{3-} + 4H^+ + H_2O + Cl^- + Na^+]^{3+}$, 759.2678 corresponding to $[\mathbf{1}^{2+} + PO_4^{3-} + 3H^+ + H_2O + Cl^- + 2Na^+]^{3+}$, and 781.2493 corresponding to $[\mathbf{1}^{2+} + PO_4^{3-} + 2H^+ + H_2O + Cl^- + 3Na^+]^{3+}$ in ESI-MS corresponded with a strong 1 : 1 complex formed between probe **1** and PO_4^{3-} anion (Fig. S6†). Therefore, the significant fluorescence intensity enhancement could be attributed to
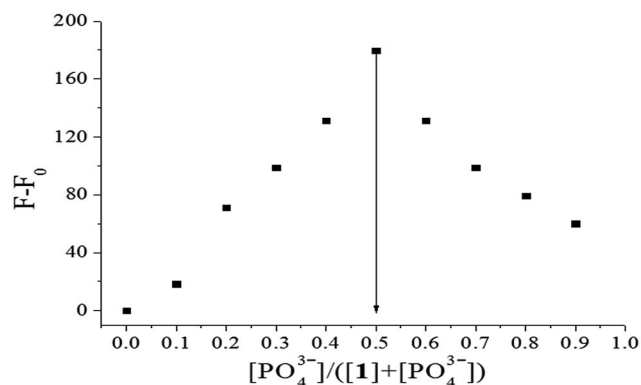
Fig. 8 Job's plot of **1** (forms 1 : 1 complex) in HEPES buffer (10 mM, pH 7.4, 25 °C) solution. F_0 and F: fluorescence maxima before and after addition of PO_4^{3-}, respectively (total concentration of **1** and PO_4^{3-} is 0.1 μM, λ_{ex} = 269 nm).

hydrogen bonding interactions between PO_4^{3-} and probe **1** in which oxygen atoms of PO_4^{3-} coordinate to the NH proton of amide and CH proton of imidazole. Moreover, hydrogen bonding interactions between amide NH protons and imidazole CH proton in the probe with oxygen atoms in PO_4^{3-} was precedented[14,20,35] and PO_4^{3-} formed three-coordinate complexes.[19]

The binding ability of probe **1** toward PO_4^{3-} was investigated using ^{1}H NMR titration experiments. Fig. 9 shows the partial ^{1}H

NMR spectra of the interaction of probe **1** and PO_4^{3-}. Free probe **1** exhibited two singlet peaks at 11.08 and 9.88 ppm in DMSO-d_6 in the far downfield region, attributed to amide H_a and imidazole H_c protons in probe **1**, respectively. With increasing of PO_4^{3-} concentrations, the singlet of H_a disappeared gradually and the signal of H_c broadened significantly through strong intramolecular hydrogen-bonding interactions in the probe and anion-ligand coordination between probe **1** and PO_4^{3-}. The disappearance of H_a was also caused by the acidity of NH, which resulted in H–D exchange in D_2O. Meanwhile, a small and definite upfield shift (0.12 ppm) for the imidazole H_c signal was observed. A small yet definite upfield shift for the H_d, H_e, and H_f signals from the aromatic units in the benzimidazolium cation occurred, from 7.72–8.14 to 7.70–8.11 ppm. This evidence showed that the high affinity of probe **1** for phosphate ions among other anions was attributed to high negative charges and the oxyacid tetrahedron that binds the coordinate complex, intermolecular hydrogen bonding interactions[36] with amide H_a and imidazole H_c, and the bis-cation was going to interact with the tris-anion through ion pairing with the anion between the two benzimidazolium units to form new host–guest complexes.

Based on the Job's plot, ESI-MS spectra, and ^{1}H NMR titration experiment results, a plausible mechanism for anion sensing is shown in Scheme 2. The energy minimized structure also shows that the amide NH proton and imidazole CH proton in [**1**–PO_4^{3-}] bind to phosphate through strong hydrogen
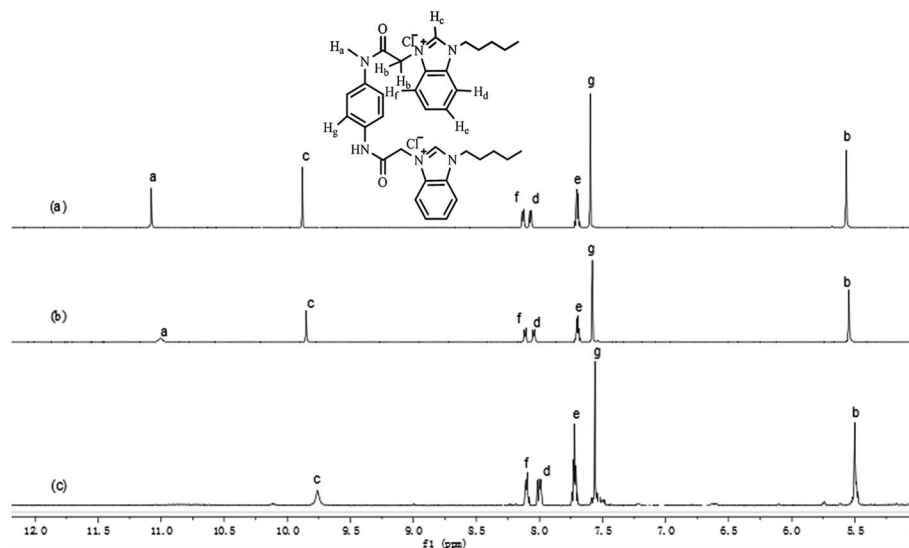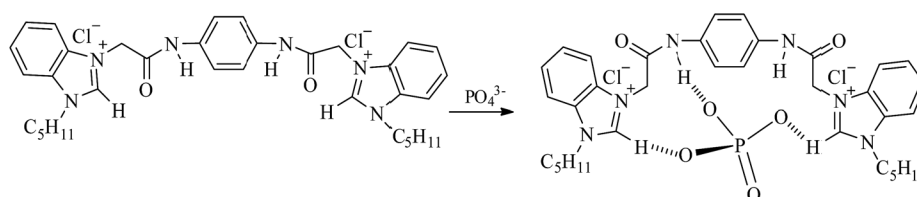

Fig. 9 Partial ^{1}H NMR spectra of probe **1** (10 μM) in DMSO-d_6 after addition of PO_4^{3-}. (a) **1**; (b) **1** + 0.5 equiv.; (c) **1** + 1.0 equiv.

Scheme 2 Proposed binding mechanism between probe **1** and PO_4^{3-}.
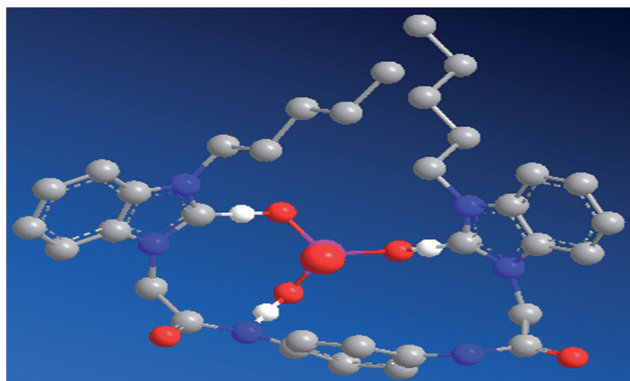
Fig. 10 Energy minimized structure of [1–PO_4^{3-}]; carbon atoms are gray, oxygen atoms are red, nitrogen atoms are blue, phosphorus atoms are pink, and hydrogen atoms are omitted for clarity.

Fig. 11 UV-vis spectra of [1–PO_4^{3-}] (10 μM) upon the addition of different metal ions (1.0 equiv.) in HEPES buffer (10 mM, pH 7.4, 25 °C) solution.

bonds. From the optimized geometry of the complex of probe **1** in Fig. 10, it was evident that the guest was strongly bound in the cleft through several hydrogen bonding interactions with both oxygen atoms of PO_4^{3-}, and amide and imidazole protons. Both the amide and imidazole protons form hydrogen bonds through $C–H^+\cdots O^-$ and $N–H^+\cdots O^-$ bonds.

3.7 Cascade recognition of [1–PO_4^{3-}] toward Fe^{3+}

Iron is one of the most abundant and versatile transition metals, and plays various important roles in many biochemical processes. There is increasing evidence that neither iron deficiencies nor excess iron induce biological disorders in the human body. Therefore, the development Fe^{3+}-selective probes with short response time, low detection limit, and low cytotoxicity is highly desirable.[22] After selective recognition with a turn-on response, 17 metal ions (Al^{3+}, Zn^{2+}, Ag^+, Ca^{2+}, Mg^{2+}, Fe^{3+}, Fe^{2+}, Hg^{2+}, Pb^{2+}, Na^+, Ba^{2+}, Ni^{2+}, K^+, Cu^{2+}, Cr^{3+}, Cd^{2+}, and Co^{2+}) were utilized to study the cascade recognition abilities of [1–PO_4^{3-}] using UV-vis absorbance spectra and fluorescence spectroscopy in HEPES buffer (pH 7.4) solution. Complex [1–PO_4^{3-}] (10 μM) was treated with 1.0 equiv. of each of the 17 metal ions, as shown in Fig. 11. Of the metal ions, only Fe^{3+} led to a noticeable increase in absorbance, a color change from colorless to light yellow, and precipitate formation after standing for 3 min, as observed by the naked eye (inset of Fig. 11). The other metal ions did not result in significant absorption changes. The selectivity of [1–PO_4^{3-}] toward Fe^{3+} was further confirmed by fluorescence spectra. As shown in Fig. 12, only 1.0 equiv. Fe^{3+} restored emission completely. In comparison, the addition of 1.0 equiv. of the other metal ions resulted in small changes. Fe^{3+} was believed to snatch PO_4^{3-} to form a stable $FePO_4$ complex due to strong electrostatic forces, which resulted in the release of free probe **1**. Apparently, the [1–PO_4^{3-}] complex can serve as a fluorescent probe in the cascade recognition, enabling its potential use in bioanalysis.

3.8 Anti-interference of [1–PO_4^{3-}] in Fe^{3+} detection

The sensing properties of fluorescence probe [1–PO_4^{3-}] toward Fe^{3+} detection were verified using competitive experiments,
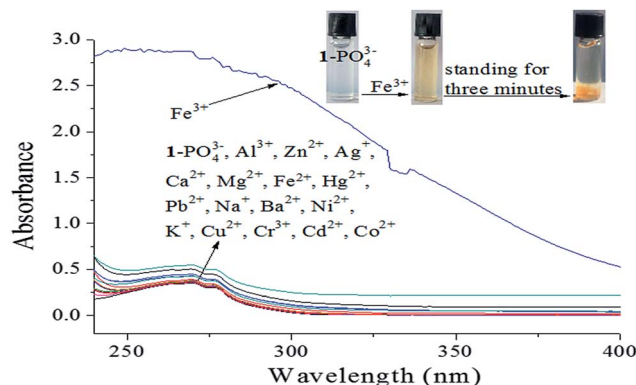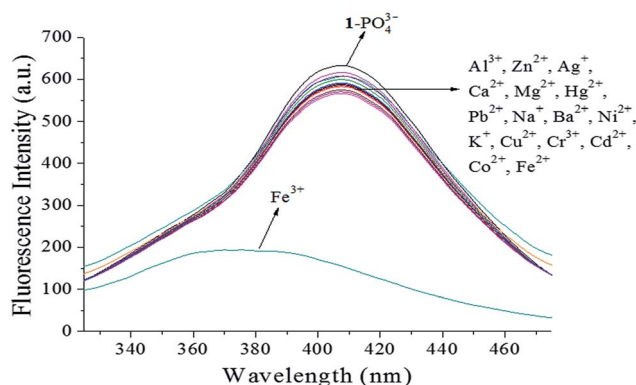

Fig. 12 Fluorescence spectra of [1–PO_4^{3-}] (10 μM) upon the addition of different metal ions (1.0 equiv.) in HEPES buffer (10 mM, pH 7.4, 25 °C) solution (λ_{ex} = 269 nm, slit = 10 nm).

which were conducted by adding 1.0 equiv. Fe^{3+} to [1–PO_4^{3-}] solution in the presence of 5.0 equiv. of other metal ions (Al^{3+}, Zn^{2+}, Ag^+, Ca^{2+}, Mg^{2+}, Fe^{2+}, Hg^{2+}, Pb^{2+}, Na^+, Ba^{2+}, Ni^{2+}, K^+, Cu^{2+}, Cr^{3+}, Cd^{2+}, and Co^{2+}). As shown in Fig. 13, the added competing ions had a negligible influence on the fluorescence maxima of [1–PO_4^{3-}] solutions in Fe^{3+} solution, which indicated the excellent anti-disturbance performance of [1–PO_4^{3-}] for monitoring Fe^{3+}.

3.9 Fluorescent titration of Fe^{3+}

The sensing ability of [1–PO_4^{3-}] toward Fe^{3+} was further determined by fluorescence titration. As shown in Fig. 14, the emission intensity of [1–PO_4^{3-}] at 409 nm decreased gradually until 1.0 equiv. of Fe^{3+} was added. The linear response of fluorescence intensity toward Fe^{3+} occurred in the Fe^{3+} concentration range 0–1.0 μM, and the linear equation was found to be $Y = 569.3283 - 103.8911X$ (linearly dependent coefficient: $R^2 = 0.9905$), as shown in Fig. 15. The detection limit, evaluated using fluorescent titration, was 0.36 nM, which was lower than the maximum level of Fe^{3+} (5.4 μM) ions permitted in drinking water by the US Environmental
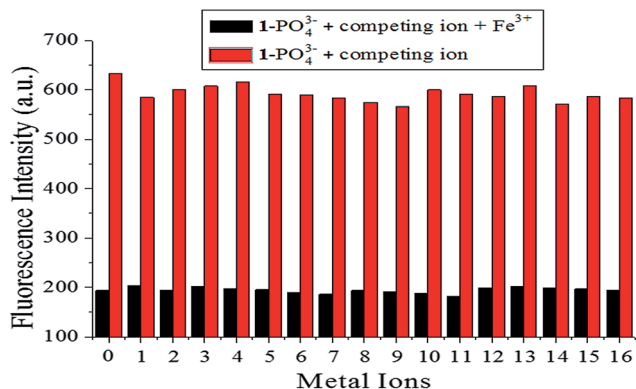
Fig. 13 Fluorescence intensity of probe [1–PO_4^{3-}] (10 μM) upon addition of various metal ions (5.0 equiv.) and Fe^{3+} (1.0 equiv.) in HEPES buffer (10 mM, pH 7.4, 25 °C) solution (λ_{ex} = 269 nm, slit = 10 nm). (0 is a blank, 1–16 represent (1) Al^{3+}, (2) Zn^{2+}, (3) Ag^+, (4) Ca^{2+}, (5) Mg^{2+}, (6) Fe^{2+}, (7) Hg^{2+}, (8) Pb^{2+}, (9) Na^+, (10) Ba^{2+}, (11) Ni^{2+}, (12) K^+, (13) Cu^{2+}, (14) Cr^{3+}, (15) Cd^{2+}, and (16) Co^{2+}.)
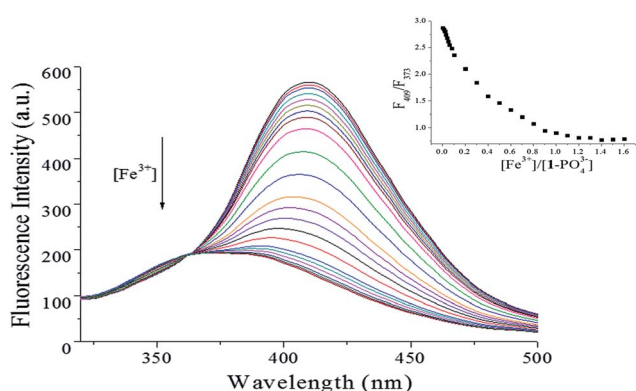

Fig. 14 Fluorescence changes in [1–PO_4^{3-}] complex (1 : 1, 10 μM) upon addition of Fe^{3+} (0–1.6 equiv.) in HEPES buffer (10 mM, pH 7.4, 25 °C) solution (λ_{ex} = 269 nm, slit = 10 nm). Insets: plot of fluorescence intensity ratio (F_{409}/F_{373}).
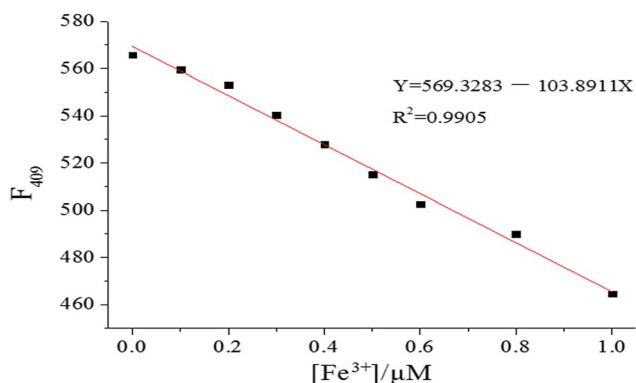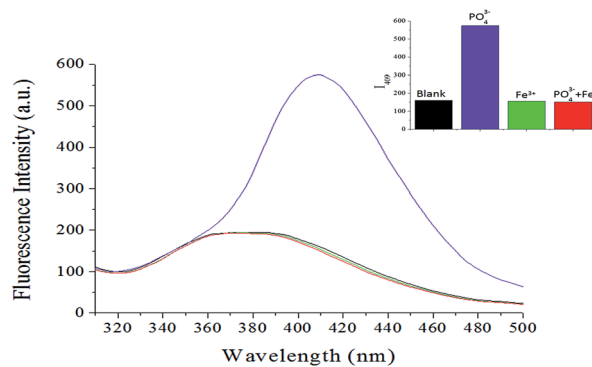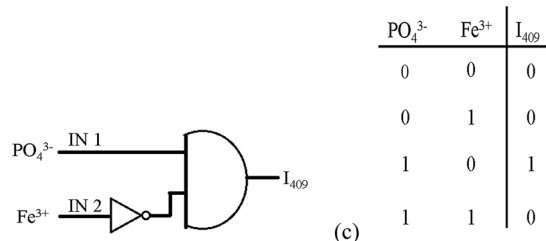

Fig. 15 Fluorescence intensity changes in [1–PO_4^{3-}] (10 μM) upon gradual addition of Fe^{3+} in HEPES buffer (10 mM, pH 7.4, 25 °C) solution (λ_{ex} = 269 nm, slit = 10 nm).

Protection Agency,[37] implying that probe [1–PO_4^{3-}] has great potential for use in the development of probe materials for Fe^{3+}.

Fig. 16 (a) Fluorescence spectra of probe 1 (10 μM) with the addition of 1.0 equiv. PO_4^{3-} ions or 1.0 equiv. Fe^{3+} ions, and the addition of 1.0 equiv. Fe^{3+} ion after 1.0 equiv. PO_4^{3-} ion; inset: fluorescence intensity at 409 nm. (b) Conventional gate notation and (c) truth table for the INH logic gate; PO_4^{3-} and Fe^{3+} ions are inputs to the system, and I_{409} is the output signal.

3.10 Molecular logic circuits

Molecular logic gates, which perform logical operations by converting inputs into detectable outputs at the molecular level, have become an active research field in supramolecular chemistry and material science because of their promising applications in molecular-scale information technology.[38,39] These systems contain binary switches to determine the output state by controlling input conditions. Due to the cascade recognition abilities of probe 1, the logic gate properties of probe 1 were studied using PO_4^{3-} ions (IN 1) and Fe^{3+} ions (IN 2) as input signals, and the fluorescence intensity at 409 nm as the output signal. The presence of PO_4^{3-} and Fe^{3+} was defined as "1" for input, and the absence of these species was defined as "0". Similarly, the "turn-on" and "turn-off" of fluorescence were defined as "1" and "0" for the output, respectively. From the perspective of logic functions, the turn-on of 1 (output "1") can be observed only in the presence of PO_4^{3-} ions (IN 1 = 1) and in the absence of Fe^{3+} ions (IN 2 = 0), as shown in Fig. 16. Under other circumstances, output "0" would be afforded due to the weak emission of 1. Therefore, probe 1 can be used as an INHIBIT (INH) logic gate[40] toward PO_4^{3-} ions in the absence of Fe^{3+} ions by observing emission at 409 nm. The pictorial representation and truth table for the corresponding INH logic gate are shown in Fig. 16b and c, respectively.

4. Conclusions

In summary, we designed and synthesized a fluorescent probe (1) for PO_4^{3-} with excellent overall performance, such as 100%

aqueous solution working medium, high selectivity and sensitivity, low detection limits (0.60 nM), strong interference immunity, favorable working pH span, and a rapid response time (10 s). A Job's plot and MS analysis showed only the formation of a $1/PO_4^{3-}$ complex with 1 : 1 stoichiometry. The binding constant of $1/PO_4^{3-}$ complex was calculated to be 2.3 × 10^5 M^{-1}. Interestingly, the resulting $[1-PO_4^{3-}]$ complex exhibited turn-off response toward Fe^{3+} ions in 100% aqueous solution, with a detection limit of 0.36 nM. The cascade recognition in the present study was used to construct an INH logic gate, which could inspire a wide range of multi-functional chemosensors based on natural products.

Acknowledgements

References

1 K. Dhanunjayarao, V. Mukundam and K. Venkatasubbaiah, *Sens. Actuators, B*, 2016, **232**, 175–180.

2 J. B. Chao, Z. Q. Li, Y. B. Zhang, F. J. Huo, C. X. Yin, H. B. Tong and Y. H. Liu, *Sens. Actuators, B*, 2016, **228**, 192–199.

3 L. M. Zhao, G. Liu and B. F. Zhang, *Spectrochim. Acta, Part A*, 2016, **169**, 45–49.

4 K. M. Xiong, F. J. Huo, C. X. Yin, Y. Y. Chu, Y. T. Yang, J. B. Chao and A. M. Zheng, *Sens. Actuators, B*, 2016, **224**, 307–314.

5 J. Tang, S. Ma, D. Zhang, Y. Q. Liu, Y. F. Zhao and Y. Ye, *Sens. Actuators, B*, 2016, **236**, 109–115.

6 G. M. Wang, H. Q. Chen, Y. Q. Chen and N. Y. Fu, *Sens. Actuators, B*, 2016, **233**, 550–558.

7 P. Ding, X. Xin, L. L. Zhao, Z. C. Xie, Q. H. Zhang, J. M. Jiao and G. Y. Xu, *RSC Adv.*, 2017, **7**, 3051–3058.

8 J. R. Jadhav, M. W. Ahmad and H. S. Kim, *Tetrahedron Lett.*, 2012, **53**, 2627–2631.

9 Y. W. Wang, S. B. Liu, Y. L. Yang, P. Z. Wang, A. J. Zhang and Y. Peng, *ACS Appl. Mater. Interfaces*, 2015, **7**, 4415–4422.

10 J. Shao, H. Lin and H. K. Lin, *Dyes Pigm.*, 2009, **80**, 259–263.

11 S. Sen, M. Mukherjee, K. Chakrabarty, I. Hauli, S. K. Mukhopadhyay and P. Chattopadhyay, *Org. Biomol. Chem.*, 2013, **11**, 1537–1544.

12 F. Albaaj and A. J. Hutchison, *Drugs*, 2003, **63**, 577–596.

13 C. Lim, M. An, H. Seo, J. H. Huh, A. Pandith, A. Helal and H. S. Kim, *Sens. Actuators, B*, 2017, **241**, 789–799.

14 Q. Y. Cao, Y. M. Han, P. S. Yao, W. F. Fu, Y. Xie and J. H. Liu, *Tetrahedron Lett.*, 2014, **55**, 248–251.

15 A. Kumar and P. S. Pandey, *Org. Lett.*, 2008, **10**, 165–168.

16 S. L. Tobey and E. V. Anslyn, *Org. Lett.*, 2003, **5**, 2029–2031.

17 F. Bartoli, A. Bencini, A. Garau, C. Giorgi, V. Lippolis, A. Lunghi, F. Totti and B. Valtancoli, *Chem.–Eur. J.*, 2016, **22**, 14890–14901.

18 G. F. Wu, Q. L. Xu, L. E. Guo, T. N. Zang, R. Tan, S. T. Tao, J. F. Ji, R. T. Hao, J. F. Zhang and Y. Zhou, *Tetrahedron Lett.*, 2015, **56**, 5034–5038.

19 I. A. Azath, P. Suresh and K. Pitchumani, *Sens. Actuators, B*, 2011, **155**, 909–914.

20 J. H. Liao, C. T. Chen and J. M. Fang, *Org. Lett.*, 2002, **4**, 561–564.

21 J. H. Xu, Y. M. Hou, Q. J. Ma, X. F. Wu and X. J. Wei, *Spectrochim. Acta, Part A*, 2013, **112**, 116–124.

22 Y. M. Liu, J. Y. Zhang, J. X. Ru, X. Yao, Y. Yang, X. H. Li, X. L. Tang, G. L. Zhang and W. S. Liu, *Sens. Actuators, B*, 2016, **237**, 501–508.

23 H. M. Chawla and T. Gupta, *Tetrahedron Lett.*, 2015, **56**, 793–796.

24 Z. G. Wang, P. Long, Y. Y. Feng, C. Q. Qina and W. Feng, *RSC Adv.*, 2017, **7**, 2810–2816.

25 J. Liu, Q. Lin, Y. M. Zhang and T. B. Wei, *Sci. China: Chem.*, 2014, **57**, 1257–1263.

26 T. Nandhini, P. Kaleeswaran and K. Pitchumani, *Sens. Actuators, B*, 2016, **230**, 199–205.

27 L. Y. Wang, Y. Zhang, L. M. Ding, J. Liu, B. Zhao, Q. G. Deng and T. Yan, *RSC Adv.*, 2015, **5**, 74764–74773.

28 B. Wannalerse, T. Tuntulani and B. Tomapatanaget, *Tetrahedron*, 2008, **64**, 10619–10624.

29 B. P. Joshi, J. Park, W. I. Lee and K. Lee, *Talanta*, 2009, **78**, 903–909.

30 H. A. Benesi and J. H. Hildebrand, *J. Am. Chem. Soc.*, 1949, **71**, 2703–2707.

31 M. J. Yuan, W. D. Zhou, X. F. Liu, M. Zhu, J. B. Li, X. D. Yin, H. Y. Zheng, Z. C. Zuo, C. B. Ouyang, H. B. Liu, Y. L. Li and D. B. Zhu, *J. Org. Chem.*, 2008, **73**, 5008–5014.

32 S. S. Zumdahl and D. C. Chemistry, *Chemical Principles*, Heath and Company, Lexington, MA, 2nd edn, 1995.

33 J. L. Sessler, J. M. Davis, V. Kral, T. Kimbrough and V. Lynch, *Org. Biomol. Chem.*, 2003, **1**, 4113–4123.

34 M. M. Hong, X. Y. Lu, Y. H. Chen and D. M. Xu, *Sens. Actuators, B*, 2016, **232**, 28–36.

35 Z. C. Xu, S. K. Kim and J. Yoon, *Chem. Soc. Rev.*, 2010, **39**, 1457–1466.

36 X. P. Bao, Y. H. Zhou and B. A. Song, *Sens. Actuators, B*, 2012, **171–172**, 550–555.

37 C. Yi, W. W. Tian, B. Song, Y. P. Zheng, Z. J. Qi, Q. Qi and Y. M. Sun, *J. Lumin.*, 2013, **141**, 15–22.

38 J. Choi, J. H. Lee and J. H. Jung, *Analyst*, 2014, **139**, 3866–3870.

39 S. Mardanya, S. Karmakar, S. Das and S. Baitalik, *Sens. Actuators, B*, 2015, **206**, 701–713.

40 J. D. Wu, X. Zhao, Y. X. Gao, J. Hu and Y. Ju, *Sens. Actuators, B*, 2015, **221**, 334–340.